Sustainable synthesis, in silico evaluation of potential toxicity and environmental fate, antioxidant and UV-filtering/photostability activity of phenolic-based thiobarbituric derivatives

Benjamin Rioux, Matthieu Mention, Jimmy Alarcan, Temitope Abiola, Cédric Peyrot, Fanny Brunissen, Albert Braeuning, Vasilios Stavros, Florent Allais

Taylor & Francis
Taylor & Francis Group

Sustainable synthesis, *in silico* evaluation of potential toxicity and environmental fate, antioxidant and UV-filtering/photostability activity of phenolic-based thiobarbituric derivatives

Benjamin Rioux, Matthieu M. Mention, Jimmy Alarcan, Temitope T. Abiola, Cédric Peyrot, Fanny Brunissen, Albert Braeuning, Vasilios G. Stavros & Florent Allais

View supplementary material

Published online: 20 Jan 2022.

Submit your article to this journal

Article views: 437

View related articles

View Crossmark data

Taylor & Francis
Taylor & Francis Group

LETTER

🔓 OPEN ACCESS   Check for updates

Sustainable synthesis, *in silico* evaluation of potential toxicity and environmental fate, antioxidant and UV-filtering/photostability activity of phenolic-based thiobarbituric derivatives

Benjamin Rioux [a], Matthieu M. Mention [a], Jimmy Alarcan[b], Temitope T. Abiola [c], Cédric Peyrot [a], Fanny Brunissen [a], Albert Braeuning[b], Vasilios G. Stavros [c] and Florent Allais [a]

aURD Agro-Biotechnologies Industrielles (ABI), CEBB, AgroParisTech, Pomacle, France; bDepartment of Food Safety, German Federal Institute for Risk Assessment, Berlin, Germany; cDepartment of Chemistry, University of Warwick, Coventry, UK

ABSTRACT

The recent ban of some organic UV-filters – such as oxybenzone or octinoxate – considered toxic for coral reef, has heightened the need for eco-friendly alternatives, especially those synthesized using green approaches that reduce the carbon footprint. In this context, several thiobarbituric acid derivatives were synthetized from bio-based *p*-hydroxybenzaldehydes (*e.g.* vanillin, syringaldehyde) through a high-yielding sustainable Knoevenagel condensation, and their UV-filtering activity, stability and antiradical properties were investigated. The results showed promising UVA and blue light coverage over time, as well as competitive EC_{50} values in comparison to commercial antioxidants (*i.e.* BHA and BHT). In order to evaluate the potential of these molecules as substitutes to current petroleum-based UV-filters, the potential toxicity and fate in environment of these new compounds were evaluated *in silico*. This screening did not show a critical potential for toxicity, making them promising candidates for further *in vitro* and *in vivo* assessment.
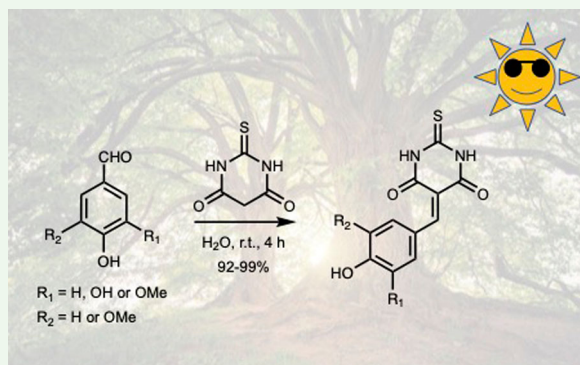
1. Introduction

To significantly decrease the carbon footprint of humans on nature, the development and use of bio-based compounds, over their petroleum-based counterparts, with low ecological impact is not only in high demand but also essential. In this context, agricultural waste comes to mind as a formidable reservoir of natural building blocks. Indeed, the valorization of undesired biomass (*e.g.* lignin, lignans) allows one to obtain sustainable aromatic building blocks such as *p*-hydroxybenzaldehydes (*i.e.* vanillin, syringaldehyde) (*1,2*). From these *p*-hydroxybenzaldehydes, a myriad of bio-based molecules can be synthesized with a wide variety of properties, such as antioxidant (*3–5*), anti-tyrosinase (*6–8*), anti-UV (*9–13*), anticancer (*14–16*) or antimicrobial (*17–19*) activities.

Recently, there have been many reports in the literature on the design of novel renewable *p*-hydroxycinnamic acids-based UV-filters and their sustainable synthesis using the Knoevenagel and Knoevenagel-Doebner condensation (*3,10,20,21*). These two reactions, which have been known for decades, originally involved

the use of pyridine as solvent and amine as catalyst (*i.e.* aniline or piperidine (*22*)). Since then, several improvements based on green chemistry principles (*23*), were carried out to reduce reaction time and limit/avoid the use of toxic solvent or catalyst (*24*). For instance, the reaction time was drastically shortened using microwave-activation (*20, 25*). Diverse procedures also report the use of dimethyl sulfoxide (DMSO (*26*)) or dimethylformamide (DMF (*27*)) as alternative solvents; however those remain hazardous for human health. Also, ionic liquids have been shown to be good replacement to pyridine as solvents (*28, 29*), nevertheless their use at industrial scale is still limited (*30*). The use of ethanol is described in a water–ethanol solvent mixture using cobalt ferrite nanoparticles as catalyst (*31*). Other catalysts were explored to substitute aniline or piperidine, including 3-aminopropylated silica gel (NAP) in water (*32*), benign amines and ammonium salts (*33*). Natural L-tyrosine showed good efficiency as a green catalyst in the solvent-free Knoevenagel condensation (*34*). Recently, green Knoevenagel condensation procedures have been used to synthesize *p*-hydroxycinnamic acids and *p*-hydroxycinnamic diacids. Here, pyridine and aniline were substituted by ethanol and L-proline as solvent and catalyst, respectively, both of which are not only safe for human health but also eco-friendly (*3, 21*). In a previous study, we described a green Knoevenagel condensation in hot water to access *p*-hydroxycinnamyl Meldrum's derivatives in the absence of catalyst (*10*).

Thiobarbituric derivatives have been reported to be studied as chemo-sensors (*35*), urease inhibitors (*36*), anticancer agents (*37, 38*), antivirals (*39*) or antioxidants (*40, 41*). However, to the best of our knowledge, thiobarbituric derivatives have never been reported as potential UV-filters. The development of new compounds involves the investigation of their potential toxicity and also their fate in the environment. In the context of compound screening, *in silico* tools represent a great approach to gain preliminary information without extensive animal testing. *In silico* models mostly rely on the principle of similarity, assuming that compounds with similar

chemical structure are expected to exert similar biological activities (*42, 43*).

In the present work, we: (1) used the aforementioned procedure to obtain *p*-hydroxycinnamyl thiobarbituric acids with an improved greener pathway, *i.e.* in the absence of heating (at room temperature) that avoids energy expenditure (Scheme 1, 92–99% yield); (2) explored their antioxidant and anti-UV properties; and (3) assessed their potential toxicity and environmental fate *in silico*.

2. Experimental

2.1. General

All reagents were purchased from Sigma–Aldrich, TCI, Merck or VWR and used as received. Solvents were purchased from Thermo Fisher Scientific and VWR. Deuterated dimethylsulfoxide (DMSO-d_6 <0.02%H_2O) was purchased from Euriso-top.

2.2. General synthetic procedure

Corresponding benzaldehydes (ca.15 mmol) and thiobarbituric acid (1 eq.) were mixed in a round-bottom flask in deionized H_2O (0.15 mol/L) and stirred at room temperature for 4 h. The resulting precipitate was filtered and freeze-dried overnight. Compounds were recovered as yellow to orange powder in excellent yields (92–99%).

2.3. NMR analyses

NMR spectra were recorded on a Bruker Fourier 300 (Billerica, MA, USA). ^1H NMR spectra were recorded in DMSO-d_6 (residual peak at δ = 2.50 ppm) at 300 MHz. Chemical shifts were reported in parts per million relative to the solvent residual peak. Data are reported as follows: integration, chemical shift (δ ppm), multiplicity (s = singlet, d = doublet and dd = doublet of doublets), coupling constant (Hz) and assignment. ^{13}C NMR spectra of
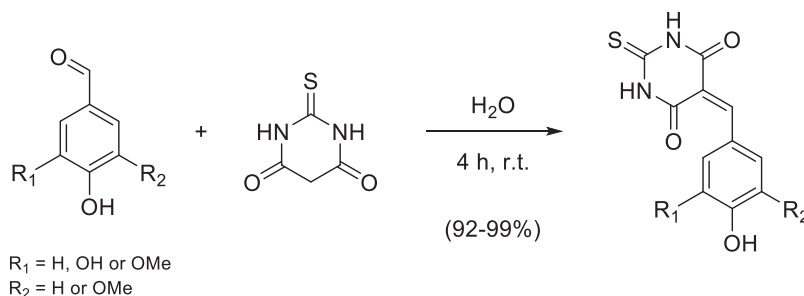
Scheme 1. General synthetic pathway to *p*-hydroxycinnamyl thiobarbituric derivatives.

samples were recorded at 75 MHz in DMSO-d_6 (residual signal at $\delta = 39.52$ ppm). Data are reported as follows: chemical shift (δ ppm) and assignment. All ^{1}H and ^{13}C NMR spectra are available in the supporting information (Figures S1–10).

2.4. Melting points and thermal stability

Melting points were recorded on a Mettler Toledo MP50 Melting Point system ($T_{initial} = 150°C$, heating 3°C / minute up to 299°C with ME-18552 sample tubes) or measured through Differential Scanning Calorimetry (DSC). DSC was performed with a DSC Q20 from TA Instruments (New Castle, DE, USA). Typically, *ca.* 8 mg sample was placed in a sealed pan, flushed with highly pure nitrogen gas and passed through heat-cool-heat cycles at 10°C.min^{-1} in a temperature range from −50°C to 200°C. The thermal stability was measured by thermogravimetric analyses (TGA) on a TA Q500 from TA Instruments (New Castle, DE, USA). Typically, *ca.* 2 mg of each sample was equilibrated at 50°C for 30 min and was flushed with highly pure nitrogen gas. All the experiments were performed with a heating rate of 10°C.min^{-1} up to 500°C. The reported values $T_{d5\%}$ and $T_{d50\%}$ represent the temperature at which 5% and 50% of the mass is lost, respectively.

2.5. HRMS analyses

High-resolution mass spectrometry was performed on an Agilent Technologies 1290 system, equipped with a 6545 Q-TOF mass spectrometer (Wilmington, DE, USA) and a PDA UV detector. The source was equipped with a JetStream ESI probe operating at atmospheric pressure. HRMS spectra are reported in the supporting information (Figures S11–15).

2.6. UV-filtering property and photostability

The UV-Vis and photostability measurements of each *p*-hydroxycinnamyl thiobarbituric derivative were taken at ~20 µM concentration (in DMSO) in a 1 cm path length quartz cuvette, using a Cary 60 Spectrometer (Agilent Technologies), both before irradiation (t_0), and at various times during 120 min irradiation (t_{120}) with an arc lamp (Fluorolog 3, Horiba). The irradiance at maximal absorption (λ_{max}) of the sample for each molecule was set so as to mimic one sun (1000 W/m^2) equivalent at Earth's surface, with an 8 nm full width half maximum (FWHM). The t_{120} UV spectrum is then compared to the original one (t_0), and the loss in absorbance is calculated at the λ_{max}. UV-Vis and photostability

spectra are reported in Figures 1–2 and in the supporting information (Figures S16–20) respectively.

2.7. Antiradical activities

To determinate the radical scavenging activity of the *p*-hydroxycinnamyl thiobarbituric derivatives, we used the 2,2-diphenyl-1-picrylhydrazyl (DPPH) assay (*44*). The analysis involved adding the candidate antiradical molecule, *i.e. p*-hydroxycinnamyl thiobarbituric derivative, in ethanol at different concentrations to homogeneous DPPH solution (also in ethanol). The study was performed for 7 hrs 25 min under stirring with the following concentration scale: 40, 20, 10, 5 and 2.5 nmol. Every 5 min, the absorbance was measured at 520 nm. At the end, the percentage curves of %DPPH (blue) and % reduced DPPH (green) were plotted in Regressi® software using an average of the last six points. The amount needed to reduce the initial number of DPPH free radicals by half (*i.e.* EC$_{50}$) was provided by the crossing point of %DPPH (blue) and %reduced DPPH (green). The lower the EC$_{50}$ value, the higher the antioxidant potential is. Antiradical measurement spectra are reported in the supporting information (Figures S21–28).

2.8. In silico toxicology and environmental fate

2.8.1. Mutagenicity and carcinogenicity

We used three different software tools to predict the mutagenicity and carcinogenicity of our selection of test compounds. The use of multiple models has proven to increase the predictive power (*45, 46*). The Toxicity Estimation Software Tool (*47*) (TEST) of the United States Environmental Protection Agency (US EPA) was employed for mutagenicity prediction. The output value for the 'Consensus Method' was used for the present study, which is the mean of the two
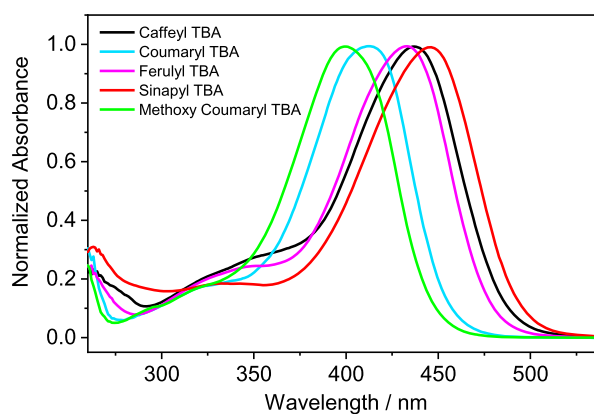

Figure 1. UV-Vis spectra of thiobarbituric acid series recorded at 20 µM in DMSO.
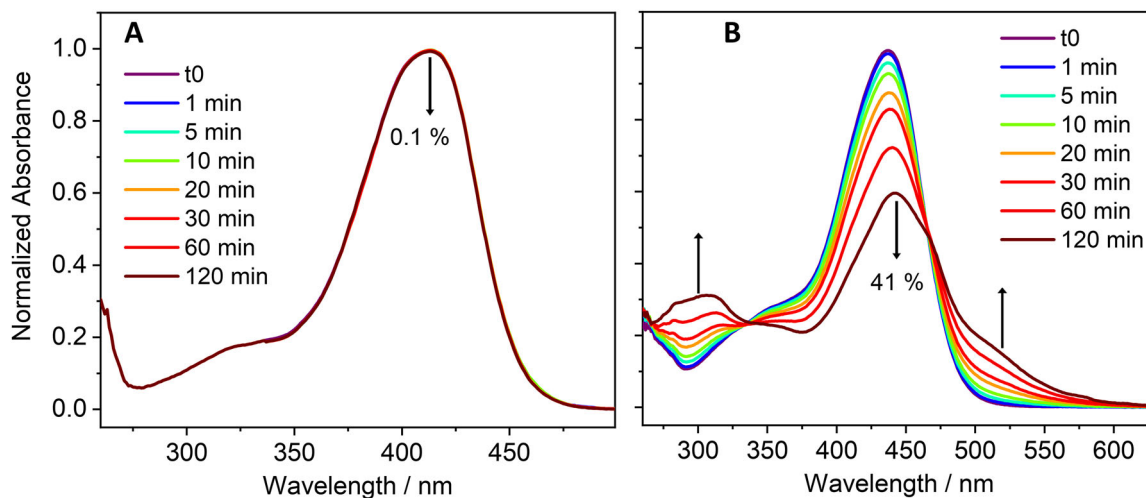
Figure 2. Long-term photostability of (A) CTBA, and (B) CafTBA. UV-Visible spectra of samples obtained in DMSO at varying duration of irradiation with a xenon arc lamp. The downward arrows denote the observed decrease in absorbance over 120 min of irradiation. The upward arrows shown in CafTBA indicates the growth of new absorbing feature following irradiation.

values obtained for the 'Hierarchical Clustering' and the 'Nearest Neighbor' methods. TEST gives a prediction in the form of a numeric value between 0 and 1, in which presumable non-mutagenicity ranges from 0 to 0.50, while mutagenicity ranges from 0.51 to 1. In addition to the TEST platform, we have also employed the VEGA (48) platform, which utilizes four models for predicting mutagenicity and carcinogenicity, together with one mutagenicity consensus model. The different models used for the endpoint mutagenicity (ISS, SARpy, CAESAR, Mutagenicity Read-Across/KNN) were built based on experimental data derived from *in vitro* studies (*e.g.* the Ames Test in Salmonella typhimurium strains), while the carcinogenicity models (ISS, ISSCAN-CGX, CAESAR, ANTARES) were derived using data from *in vivo* studies in different species, mainly mice and rats. The VEGA models generate an output with a 'yes' or 'no' prediction with regard to the respective endpoint, plus information about the reliability of the prediction (low, moderate, or high reliability). In order to compare the outcomes with the predictions generated by other models, the wording of the VEGA predictions was translated into a so-called mutagenicity or carcinogenicity score, which is a numeric value between 0 and 1, where 0 stands for no toxic (*i.e.* non-mutagenic or non-carcinogenic) potential and 1 stands for strong toxicity potential. The classification for the graded translation is given in Table 1. For the mutagenicity consensus model, the calculation is different as a value is already provided by VEGA, ranging from 0 to 1. In case the test compound is predicted as non-mutagenic, the given value must be re-scaled to fit to the graduation described in Table 1. Therefore, non-mutagenicity values were

re-scaled using the following calculation:

$$score = \frac{(1 - \boldsymbol{x}) \times 0.5}{0.9}$$

with x the value given by VEGA for the mutagenicity consensus model.

In case the test compound is predicted as mutagenic, the given value is re-scaled using the following calculation:

$$score = 1 - \frac{(1 - \boldsymbol{x}) \times 0.5}{0.9}$$

with x is the value given by VEGA for the mutagenicity consensus model.

The open source software LAZAR (49) includes different endpoints for the evaluation of the toxicity of substances based on their structure. The three models 'Rat,' 'Mouse,' and 'Rodents (multiple species/sites)' were used for carcinogenicity prediction, and '*Salmonella typhimurium*' was used for mutagenicity prediction. The output of the LAZAR models occurs in the form of an

Table 1. Translation of the VEGA predictions into a mutagenicity/carcinogenicity score.

Prediction	Reliability	Score
mutagenic/carcinogenic	experimental data	1
mutagenic/carcinogenic	good reliability	0.9
possible mutagenic/carcinogenic	good reliability	0.8
mutagenic/carcinogenic	moderate reliability	0.7
possible mutagenic/carcinogenic	moderate reliability	0.6
(possible) mutagenic/carcinogenic	low reliability	0.5
(possible) non-mutagenic/non-carcinogenic	low reliability	0.5
possible non-mutagenic/non-carcinogenic	moderate reliability	0.4
non-mutagenic/non-carcinogenic	moderate reliability	0.3
possible non-mutagenic/non-carcinogenic	good reliability	0.2
non-mutagenic/non-carcinogenic	good reliability	0.1
non-mutagenic/non-carcinogenic	experimental data	0

'active/non-active' statement combined with a probability score. The predictions of the three LAZAR carcinogenicity models were combined and translated into a single carcinogenicity score as follows: starting from a virtual value of 0.5, a value of 0.133 was added to this value for every model that predicted the respective compound to be 'carcinogenic,' while a value of 0.133 was subtracted for every model yielding the prediction 'non-carcinogenic.' Thus, in the case that all three models predicted a compound to be carcinogenic, the final value would be 0.9, and in the case that all three models yielded the same prediction 'non-carcinogenic' for a given compound, the final value would be 0.1. For mutagenicity prediction, the given probability was used to determine the score. A probability value higher than 0.66 was considered equal to the 'good reliability' of the VEGA predictions and is attributed the score of 0.1 or 0.9 depending on the negative or positive prediction. A probability value lower than 0.33 was considered equal to the 'low reliability' of the VEGA predictions and is attributed the score of 0.5. A probability value comprised between 0.33 and 0.66 was considered equal to the 'moderate reliability' of the VEGA predictions and is affected the score of 0.3 or 0.7 depending on the negative or positive prediction.

To obtain a single mutagenicity or carcinogenicity score, the arithmetic mean of the different generated prediction scores was calculated and interpreted as follows: a score higher than 0.66 means a positive prediction (mutagenic or carcinogenic) with good reliability; a score lower than 0.33 means a negative prediction (mutagenic or carcinogenic) with good reliability; a score comprised between 0.33 and 0.66 is considered equivocal: $0.33 <$ score ≤ 0.5 is regarded as negative prediction (mutagenic or carcinogenic) but with insufficient reliability, and $0.5 \leq$ score < 0.66 is regarded as positive prediction (mutagenic or carcinogenic) but with insufficient reliability.

2.8.2. Endocrine toxicity

The VEGA platform was further used to investigate the endocrine toxicity of the test compounds. In total, 5 models were employed: one that estimates receptor binding affinity (Estrogen Receptor Relative Binding Affinity model IRFMN) and four that predict receptor-mediated effects (Estrogen Receptor-mediated effect IRFMN/CERAPP, Androgen Receptor-mediated effect IRFMN/COMPARA, Thyroid Receptor Alpha effect NRMEA, and Thyroid Receptor Beta effect NRMEA). Each model yields both a qualitative prediction (yes/no) and information about the reliability of the prediction (low, moderate, or high reliability).

2.8.3. Acute and short-term toxicity

The oral LD_{50} and no-observed-adverse-effect levels (NOAEL) from 90-day toxicity studies were chosen as representative endpoints for acute and short-term toxicity. Estimation of oral LD_{50} in rat was provided by TEST using the Nearest neighbor method, which is based on a dataset comprising values from 7413 substances. The prediction of the NOAEL was made using the module NOAEL – IRFMN/CORAL provided by the VEGA platform. This model is based on a dataset comprising values from repeated-dose 90-days oral toxicity studies in rodents with 140 substances.

2.8.4. Bioaccumulation

Bioaccumulation was evaluated using the bioconcentration factor (BCF), which is defined as the ratio of the concentration of the test chemical in aquatic organisms to its concentration in the ambient environment. The VEGA platform provides 4 models for the prediction of BCF (CAESAR, Meylan, KNN/Read-across, and Arnot-Gobas). For each model, a log value is given, plus information about the reliability of the prediction (low, moderate, or high). Additionally, BCF was evaluated using the online tool ISIDA/Predictor (50) from the Laboratory of Chemoinformatics website provided by the University of Strasbourg. ISIDA is a consensus regression model based on 17 individual models. The outcome is given as log value with a prediction confidence estimate (outside applicability domain (AD), average, good, and optimal). According to the Registration, Evaluation, Authorisation and Restriction of Chemicals (REACH) regulation, a substance with a BCF higher than 2000 (or log BCF > 3.3) is considered bioaccumulative, while a substance with a BCF higher than 5000 (or log BCF > 3.7) is considered very bioaccumulative.

2.8.5. Biodegradability

Biodegradability was evaluated using the IRFMN model provided by the VEGA platform. Similar to mutagenicity predictions, the outcome is given as qualitative prediction (readily biodegradable/not readily biodegradable), plus information about the reliability of the prediction (low, moderate, or high reliability). In addition, we used the online tool ISIDA/Predictor that provides a consensus regression model based on 15 individual models. The outcome is given as a statement (readily biodegradable/not readily biodegradable) with a prediction confidence estimate (outside AD, average, good, and optimal).

2.8.6. Persistence

Persistence in sediment, soil, and water were evaluated using the qualitative and quantitative IRFMN models

provided by the VEGA platform. The qualitative model gives a statement (not persistent or nP, close to persistence threshold or nP/P, close to very persistent threshold or P/vP, very persistent or vP) with information on the reliability of the prediction (low, moderate, or high reliability), while the quantitative model gives an estimate on the number of days of persistence in the so-called matrix, also with information on the reliability of the prediction. Additionally, we used the online tool ISIDA/Predictor that provides a consensus model based on 19, 15, and 20 individual models, respectively. The outcome is given as a statement (persistent P or not persistent nP) with a prediction confidence estimate (outside AD, average, good, and optimal). In order to compare the predictions from the three different models, the wording of the VEGA and ISIDA predictions were translated into a so-called persistence score that is a numeric value between 0 and 1, where 0 stands for not persistent and 1 stands for persistent. The classification for the graded translation is given in Tables 2 and 3. To ease the classification of the VEGA predictions, the four different outcomes in the qualitative models were grouped into two main classes: not persistent (nP and nP/P) and persistent (P/vP and vP). The outcomes in the quantitative models were assigned a score depending if they were higher or lower than the respective threshold of 120 days for persistence in sediment and soil or the threshold of 40 days for persistence in water.

**Table 2.** Translation of the VEGA predictions into a persistence score.

VEGA prediction	Reliability	Score
persistent	experimental data	1
P/vP or vP or >120 days or >40 days	good reliability	0.9
P/vP or vP or >120 days or >40 days	moderate reliability	0.7
P/vP or vP or >120 days or >40 days	low reliability	0.5
nP or nP/P or <120 days or <40 days	low reliability	0.5
nP or nP/P or <120 days or <40 days	moderate reliability	0.3
nP or nP/P or <120 days or <40 days	good reliability	0.1
non-persistent	experimental data	0

**Table 3.** Translation of the ISIDA predictions into a persistence score.

ISIDA prediction	Reliability	Score
persistent	experimental data	1
persistent	optimal reliability	0.9
persistent	good reliability	0.766
persistent	average reliability	0.633
persistent	outside AD	0.5
non-persistent	outside AD	0.5
non-persistent	average reliability	0.366
non-persistent	good reliability	0.233
non-persistent	optimal reliability	0.1
non-persistent	experimental data	0

Similar to the mutagenicity/carcinogenicity score, the arithmetic mean of the different generated prediction scores was calculated and interpreted as follows: a score higher than 0.66 means a positive prediction (persistent) with good reliability; a score lower than 0.33 means a negative prediction (not persistent) with good reliability; a score between 0.33 and 0.66 is considered equivocal: $0.33 < score \leq 0.5$ is regarded a negative prediction (not persistent) but with insufficient reliability, and $0.5 \leq score < 0.66$ is regarded a positive prediction (persistent), but with insufficient reliability.

2.9. Experimental descriptions
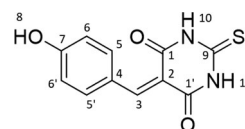
Coumaryl thiobarbituric acid (CTBA): filtration led to a yellow orange powder (92%); **m.p.** 199°C; **UV:** λ_{max} (DMSO, nm) 414, ε (L.mol^{-1}.cm^{-1}) 32,200. **^{1}H NMR** (300 MHz, 25°C, DMSO-d$_6$) δ: 12.35 and 12.26 (2H, 2s, H-10 and H-10′), 10.98 (1H, s, H-8), 8.38 (2H, d, $J = 9.0$ Hz, H-5 and H-5′), 8.22 (1H, s, H-3), 6.89 (2H, d, $J = 8.9$ Hz, H-6 and H-6′). **^{13}C NMR** (75 MHz, 25°C, DMSO-d$_6$) δ: 178.2 (C-9), 163.8 (C-7), 162.5 and 160.1 (C-1 and C-1′), 156.6 (C-3), 138.9 (C-5 and C-5′), 124.0 (C-4), 115.7 (C-6 and C-6′), 114.3 (C-2). **TOF MS ES+**: [M + H]$^+$ for C$_{11}$H$_9$N$_2$O$_3$S: m/z 249.0334; found: m/z 249.0335.
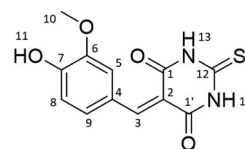
Ferulyl thiobarbituric acid (FTBA): filtration led to an orange powder (99%); **m.p.** 151°C; **UV:** λ_{max} (DMSO, nm) 433, ε (L.mol^{-1}.cm^{-1}) 33,200. **^{1}H NMR** (300 MHz, 25°C, DMSO-d$_6$) δ: 12.37 and 12.27 (2H, 2s, H-13 and H-13′), 10.78 (1H, s, H-11), 8.50 (1H, d, $J = 2.1$ Hz, H-5), 8.24 (1H, s, H-3), 7.88 (1H, dd, $J = 2.1$ Hz and $J = 8.6$ Hz, H-9), 6.92 (1H, d, $J = 8.4$ Hz, H-8), 3.83 (3H, s, H-10). **^{13}C NMR** (75 MHz, 25°C, DMSO-d$_6$) δ: 178.1 (C-12), 162.5 and 160.3 (C-1 and C-1′), 157.0 (C-3), 154.0 (C-7), 147.1 (C-6), 133.3 (C-9), 124.5 (C-4), 118.3 (C-5), 115.5 (C-8), 114.1 (C-2), 55.6 (C-10). **TOF MS ES+**: [M + H]$^+$ for C$_{12}$H$_{11}$N$_2$O$_4$S: m/z 279.0440; found: m/z 279.0438.
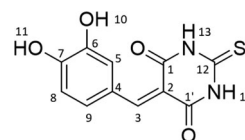
Caffeyl thiobarbituric acid (CafTBA): filtration led to an orange powder (93%); **m.p.** 169°C; **UV:** λ_{max} (DMSO, nm) 439, ε (L.mol^{-1}.cm^{-1}) 38,800. **^{1}H NMR** (300 MHz, 25°C, DMSO-d$_6$) δ: 12.33 and 12.25 (2H, 2s, H-13 and H-13'), 8.29 (1H, d, $J = 2.2$ Hz, H-5), 8.13 (1H, s, H-3), 7.67 (1H, dd, $J = 2.2$ Hz and $J = 8.6$ Hz, H-9), 6.87 (1H, d, $J = 8.4$ Hz, H-8). **^{13}C NMR** (75 MHz, 25°C, DMSO-d$_6$) δ: 178.2 (C-12), 162.6 (C-1), 160.1 (C-1'), 157.1 (C-3), 153.3 (C-7), 145.1 (C-6), 132.4 (C-9), 124.5 (C-4), 121.4 (C-5), 115.6 (C-8), 113.7 (C-2). **TOF MS ES+**: [M + H]$^+$ for C$_{11}$H$_9$N$_2$O$_4$S: m/z 265.0283; found: m/z 265.0280.
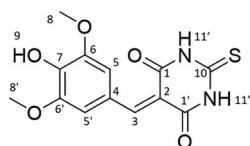
Sinapyl thiobarbituric acid (STBA): filtration led to an orange powder (95%); **m.p.** non-determined, 5% thermo-degradation: **T$_{d5\%}$** = 287°C; **UV:** λ_{max} (DMSO, nm) 445, ε (L.mol^{-1}.cm^{-1}) 37,800. **^{1}H NMR** (300 MHz, 25°C, DMSO-d$_6$) δ: 12.38 and 12.27 (2H, 2s, H-11 and H-11'), 10.28 (1H, 1s, H-9), 8.28 (1H, s, H-3), 8.07 (2H, s, H-5 and H-5'), 3.84 (6H, s, H-8 and H-8'). **^{13}C NMR** (75 MHz, 25°C, DMSO-d$_6$) δ: 178.1 (C10), 162.6 and 160.3 (C-1 and C-1'), 157.4 (C-3), 147.2 (C-6 and C-6'), 143.4 (C-7), 123.0 (C-4), 114.3 (C-5 and C-5'), 114.3 (C-2), 56.1 (C-8 and C-8'). **TOF MS ES+**: [M + H]$^+$ for C$_{13}$H$_{13}$N$_2$O$_5$S: m/z 309.0545; found: m/z 309.0544.
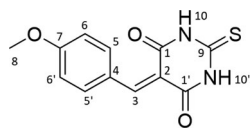
4-methoxycoumaryl thiobarbituric acid (MeCTBA): filtration led to a yellow orange powder (99%); **m.p.** 264–268°C; **UV:** λ_{max} (DMSO, nm) 399, ε (L.mol^{-1}.cm^{-1}) 30,200. **^{1}H NMR** (300 MHz, 25°C, DMSO-d$_6$) δ: 12.40 and 12.30 (2H, 2s, H-10 and H-10'), 8.42 (2H, d, $J = 9.0$ Hz, H-5 and H-5'), 8.26 (1H, s, H-3), 7.08 (2H, d, $J = 8.8$ Hz, H-6 and H-6'), 3.88 (3H, s, H-8). **^{13}C NMR** (75 MHz, 25°C, DMSO-d$_6$) δ: 178.3 (C-9), 164.0 (C-7), 162.3 and 160.0 (C-1 and C-1'), 156.0 (C-3), 138.0 (C-5 and C-5'), 125.3 (C-4), 115.7 (C-2), 114.1 (C-6 and C-6'), 55.8 (C-8). **TOF MS ES+**: [M + H]$^+$ for C$_{12}$H$_{10}$N$_2$O$_3$S: m/z 263.0490; found: m/z 263.0490.

3. Results

3.1. Synthesis

Based on our previous findings on bio-based diethyl sinapate and Meldrum's p-hydroxycinnamic acids based UV-filters (10, 12), we decided to extend this strategy by synthesizing potential UV-filters substituted with thiobarbituric acid moieties, with the goal that the use of nitrogen and sulfur atoms would shift the UV spectra into the visible (blue) region of the electromagnetic spectrum (380–500 nm) (51). To access these phenolic-based thiobarbituric derivatives through the greenest possible synthetic procedure, we attempted to conduct the Knoevenagel condensation in water without adding any catalyst, to avoid the use of toxic organic solvent while improving atom economy, as already described in previous work (10, 52). Moreover, the reaction was performed at room temperature to reduce energy consumption. This straightforward room temperature, catalyst- and organic solvent-free Knoevenagel condensation of p-hydroxybenzaldehydes and thiobarbituric acid resulted in excellent yields (92–99%). It is noteworthy to mention that the p- hydroxycinnamyl thiobarbituric derivatives readily precipitated from the reaction medium, thus significantly simplifying their recovery and purification through a classic filtration, while avoiding the use of energy- and solvent-consuming silica gel chromatography. We add that the synthesis of caffeyl thiobarbituric acid (CafTBA) was first performed under air but, contrary to the other molecules, led to lower yield (70%), most likely due to the presence of the two readily oxidizable -OH groups on the aromatic ring (53) leading to unwanted side reactions. To avoid this, the syntheses were performed under N$_2$ to limit this potential oxidation and this resulted in a 93% yield.

The structures of the p-hydroxycinnamic acids-based thiobarbituric acid derivatives was confirmed by ^{1}H and ^{13}C NMR spectrometry as well as high resolution mass spectrometry (see Supporting Information Figures S1–S15).

3.2. UV-filtering property and photostability

The UV-visible spectra of the p-hydroxycinnamyl thiobarbituric derivatives obtained in DMSO are reported in Figure 1. All compounds exhibited a broadband (from UV to visible region) and strong absorption profile having molar extinction coefficients ranging from ~30,000 to ~39,000 L.mol^{-1}.cm^{-1} at the λ_{max} (see experimental description). The λ_{max} of all the thiobarbituric derivatives were in the region of 400–500 nm,

except the methoxy coumaryl thiobarbiturics which peaked in the UVA (399 nm) region. This hypsochromic shift of *p*-hydroxycinnamyl derivatives, resulting from the use of a methyl protective group on the phenol, was already highlighted in a previous study (*9*).

The photostability of these molecules were also explored in DMSO. The results presented in Figure 2 and summarized in Table 4 revealed that all the *p*-hydroxycinnamyl thiobarbiturics, except the caffeyl derivative, were photostable, revealing only minor (< 5%) reduction in sample absorbance at λ_{max} over two hours of irradiation. Caffeyl thiobarbituric acid on the other hand, showed a significant reduction (41%) in the λ_{max} together with observable increase in the spectrum both in the ~300 and ~525 nm regions, suggesting that caffeyl thiobarbituric acid is unstable towards long-term exposure to UV-visible radiation, which can be explained by the presence of the two easily oxidizable hydroxyl groups on the aromatic ring, as previously described (*53*). The high photostability of the other derivatives studied herein is promising for the design and development of new broadband sunscreens as there are less efficient UVA sunscreens on the market. For example, oxybenzone, a commonly employed broadband UV-filter is not only photo-unstable (*54*), but also considered toxic to coral reef and hence banned from sale and distribution in some Pacific Islands, such as Hawaii (*55*). This calls for development of new broadband UV-filters, and the thiobarbiturics reported herein could be of use.

3.3. In silico toxicology and environmental fate

As shown in Figure 3, most mutagenicity scores were below 0.5, but above the threshold of 0.33. This indicates that the test compounds are predicted to be non-mutagenic but the reliability of the predictions is not optimal. However, FTBA showed a score below the threshold indicating that this compound is predicted to be non-mutagenic with a good reliability. All carcinogenicity scores were between the thresholds, thus no reliable predictions could be made for these compounds (Figure 3). Available experimental data on the

Table 4. UV-Vis properties of *p*-hydroxycinnamyl thiobarbituric derivatives.

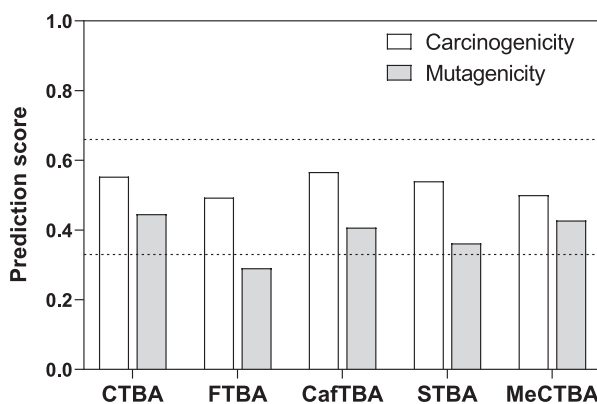| Compounds	λ_{max} (nm)	Loss in Absorbance at λ_{max} (%)
CTBA	414	0.1
FTBA	433	0.1
CafTBA	439	41
STBA	445	4.6
MeCTBA	399	0.2

Figure 3. Schematic presentation of the results of the *in silico* analysis, with regard to the endpoints mutagenicity and carcinogenicity. The test compounds are shown with their average prediction score. In addition, the prediction scores were divided in three different groups (indicated by dashed lines): the probable mutagens/carcinogens with scores greater than 0.66, the probably non-mutagens/non-carcinogens with scores smaller than 0.33 and the remaining equivocal predictions with scores between 0.33 and 0.66.

structurally related drug phenobarbital (PB) can help to circumvent this equivocal prediction outcome. PB has been used considerably in the twentieth century as oral drug to treat epilepsy, convulsions and other neurological diseases (*56*), and is still included in the WHO model list of essential medicines (*57*). In the monograph published by the IARC, PB was concluded to be non-genotoxic, but to induce adenomas in the livers of mice (*58*). Further studies showed that PB induces tumors through the activation of the constitutive androstane receptor (CAR) (*59*). Another study even showed a dual role of PB being able to either promote or inhibit hepatocarcinogenesis depending on the biological context (*60*). This specific CAR-mediated mode of action for carcinogenicity is considered not plausible for humans by many researchers, and data from different epidemiological studies conducted in humans who had been chronically exposed to PB also showed no clear evidence for an increased liver tumor risk (*59*). Therefore, it can be assumed that the test compounds are unlikely to present carcinogenic properties in humans.

Regarding endocrine toxicity, none of the test compounds were predicted to exert effects on estrogen or thyroid receptors (all predictions with good reliability) (Table S1). However, they were predicted active in regards to the androgen receptor (AR), with low or moderate reliability. Those outcomes need to be nuanced as PB (which is part of the dataset) is considered inactive with respect to AR. Therefore, these predictions might not be of biological relevance and need to be confirmed by experimental data. Only CafTBA was

predicted to have binding affinity for the estrogen receptor (ER), but the reliability was low. Since PB is experimentally inactive with respect to ER, this prediction does not raise concern.

Oral LD_{50} and NOAEL in rats were used as representative endpoints for acute and short-term toxicity (90-days study). The estimated values for LD_{50} were between 600 and 3200 mg/kg bw, while the estimated NOAELs ranged between 0.5 and 2 mg/kg bw per day (Table 5). The predicted oral LD_{50} values (over 600 mg/kg bw in average) do not indicate strong acute toxicity of the compounds, and are above the experimentally determined LD_{50} of PB (162 mg/kg bw).

As presented in Table S2, all test compounds showed a log BCF < 3.3 (with good reliability for ISIDA), indicating that they are not predicted to be bioaccumulative.

All test compounds were predicted to be readily biodegradable according to VEGA (low reliability), while ISIDA predicted all compounds not readily biodegradable (average prediction confidence). Therefore, a firm conclusion cannot be drawn regarding the biodegradability of the test compounds.

All sediment and water persistence scores were below 0.5 but above the threshold of 0.33, indicating that the test compounds are predicted to be non-persistent in sediment and water but the reliability of the predictions is not optimal (Figure 4). Soil persistence scores were very close to the threshold of 0.33 for all compounds except STBA. Thus, it is expected that those compounds are not persistent in soil.

3.4. Antiradical activities

Antioxidants are necessary for protection against reactive oxygen species (ROS), naturally induced in the body by biochemical reactions or from exogenous stimulation such as UV irradiation (61). An interesting feature for UV-filters would be to have both good photostability and antioxidant activity, so they could not only protect against the cause (UVs) but also against the resulting ROS and related skin problems resulting from solar over exposition (i.e. photoaging, inflammation, carcinogenesis (62)). In this way, the antioxidant capacities of the p-hydroxycinnamyl thiobarbituric derivatives
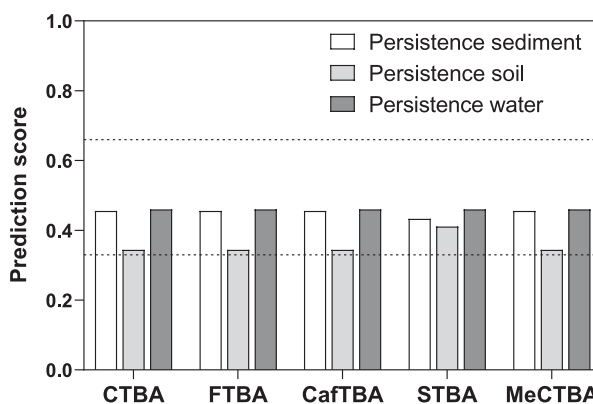

Figure 4. Schematic presentation of the results of the *in silico* analysis with regard to the endpoint persistence (sediment, soil, and water). The test compounds are shown with their average prediction score. In addition, the prediction scores were divided in three different groups (dashed lines): the probable persistent substances with scores greater than 0.66, the probably non-persistent substances with scores smaller than 0.33 and the remaining equivocal predictions with scores between 0.33 and 0.66.

were investigated as phenols – especially caffeyl and sinapyl esters and analogues – are widely recognized as good antioxidant agents thanks to their ability to quench free radicals (3, 63). As an example, the antiradical analysis of CTBA is shown in Figure 5.

Results for all *p*-hydroxycinnamyl thiobarbituric derivatives are given in Table 6 and are benchmarked against two commercially available antioxidants, BHA and BHT, and against the parent acid, *i.e.* thiobarbituric acid (TBA). EC_{50} values for BHA, BHT and TBA are 4.2, 4.1 and 3.4 nmol, respectively. For *p*-hydroxycinnamyl thiobarbituric derivatives, the caffeyl moiety (CafTBA) exhibits the best antioxidant activity with an EC_{50} of 1.9 nmol. Ferulyl (FTBA) and sinapyl (STBA) derivatives also showed promising potential with EC_{50} of 2.4 and 2.5 nmol, respectively. Finally, 4-methoxycoumaryl (MeCTBA) and coumaryl (CTBA) derivatives exhibited higher EC_{50} (4.1 and 5.8 nmol, respectively). In summary, with regards to antioxidant activity, the phenolic moieties can be ranked as follows: caffeyl > sinapyl > ferulyl > 4-methyl-coumaryl > coumaryl. It is noteworthy to mention that three *p*-hydroxycinnamyl thiobarbituric derivatives (*i.e.* CafTBA, FTBA and STBA) showed better antioxidant activity compared to the parent acid (TBA) and the two commercially available antioxidants, BHA and BHT. It suggests a synergic effect between the phenolic and the thiobarbituric moieties to provide impressive antioxidant activities. In the case of CTBA and MeCTBA, the EC_{50} values were a bit higher than thiobarbituric acid, showing an expected negative effect of those phenolic moieties on the

Table 5. Predicted oral LD_{50} and NOAEL in rats.

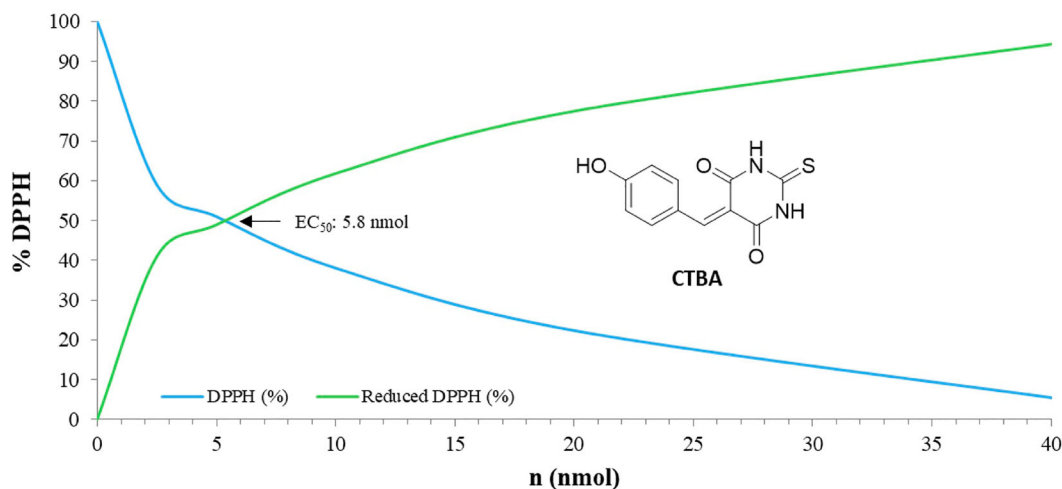| Substance	LD_{50} (mg/kg bw)	NOAEL (mg/kg bw per day)
CTBA	3124	0.95
FTBA	615	1.20
CafTBA	654	2.15
STBA	649	1.51
MeCTBA	1560	0.53

Figure 5. Determination of the antiradical activity of CTBA.

Table 6. Antiradical activities of *p*-hydroxycinnamyl thiobarbituric derivatives.

Compounds	EC$_{50}$ (nmol)	Standard Error of Mean (SEM)
CTBA	5.8	0.3
FTBA	2.4	0.0
CafTBA	1.9	0.0
STBA	2.5	0.1
MeCTBA	4.1	0.3
ThioBarbituric Acid (TBA)	3.4	0.6
ButylHydroxyAnisole (BHA)	4.2	0.1
ButylHydroxyToluene (BHT)	4.1	0.1

antiradical activities of TBA, coumaryl derivatives being known for their lack of antiradical activities (*3*, *6*, *10*, *17*). Despite this negative effect, EC$_{50}$ values were still similar to the benchmarks (BHA and BHT), consequently, thiobarbituric acid could be used to engineer antiradical compounds bearing coumaryl moieties or other molecular moieties with no innate antiradical activities.

4. Conclusions

Herein, we report a high-yielding new and green synthetic pathway to bio-based *p*-hydroxycinnamyl thiobarbituric derivatives. The study of their UV properties and photostability showed the potential of such compounds to protect against UVA and blue light with high levels of photostability over prolonged irradiation. Moreover, the native antiradical property of thiobarbituric acid yielded compounds with EC$_{50}$ values comparable with compounds commonly used in the industry (*i.e.* BHA and BHT). Considering the present *in silico* data, the test compounds do not show a critical potential for toxicity. The candidate compounds might therefore be suited for further development regarding their intended purpose

of use. Nonetheless, it should be pointed out that *in silico* approaches, despite their usefulness in early compound development and prioritization, are not yet able to replace biological testing *in vitro* and/or *in vivo*. Thus, proper toxicological examination will still be required for admission of the test compounds to the market. Such studies are, however, beyond the scope of this study.

ORCID

Benjamin Rioux http://orcid.org/0000-0002-4954-1380
Matthieu M. Mention http://orcid.org/0000-0002-2309-9870
Temitope T. Abiola http://orcid.org/0000-0003-3723-4962
Cédric Peyrot http://orcid.org/0000-0001-8843-6498
Fanny Brunissen http://orcid.org/0000-0002-0357-4670
Vasilios G. Stavros http://orcid.org/0000-0002-6828-958X
Florent Allais http://orcid.org/0000-0003-4132-6210

References

[1] Rais, D.; Zibek, S. *Adv. Biochem. Eng./Biotechnol.* **2019,** *166*, 469–518. doi:10.1007/10_2017_6.

[2] Setyaningsih, W.; Saputro, I.E.; Carrera, C.A.; Palma, M. *Food Chem.* **2019,** *288*, 221–227. doi:10.1016/j.foodchem.2019.02.107.

[3] Rioux, B.; Peyrot, C.; Mention, M.M.; Brunissen, F.; Allais, F. *Antioxidants* **2020,** *9*, 331. doi:10.3390/antiox9040331.

[4] Mouterde, L.M.M.; Peru, A.A.M.; Mention, M.M.; Brunissen, F.; Allais, F. *J. Agric. Food Chem.* **2020,** *68*, 6998–7004. doi:10.1021/acs.jafc.0c02183.

[5] Kozlowski, D.; Trouillas, P.; Calliste, C.; Marsal, P.; Lazzaroni, R.; Duroux, J.-L. *J. Phys. Chem. A* **2007,** *111*, 1138–1145. doi:10.1021/jp066496+.

[6] Minsat, L.; Peyrot, C.; Brunissen, F.; Renault, J.-H.; Allais, F. *Antioxidants* **2021,** *10*. doi:10.3390/antiox10040512.

[7] Liu, J.; Chen, C.; Wu, F.; Zhao, L. *Chem. Biol. Drug Des.* **2013,** *82*, 39–47. doi:10.1111/cbdd.12126.

[8] Lee, S.Y.; Baek, N.; Nam, T.-g. *J. Enzyme Inhib. Med. Chem.* **2016,** *31*, 1–13. doi:10.3109/14756366.2015.1004058.

[9] Peyrot, C.; Mention, M.M.; Brunissen, F.; Allais, F. *Antioxidants* **2020,** *9*. doi:10.3390/antiox9090782.

[10] Peyrot, C.; Mention, M.M.; Brunissen, F.; Balaguer, P.; Allais, F. *Molecules* **2020,** *25*, 2178. doi:10.3390/molecules25092178.

[11] Mention, M.M.; Flourat, A.L.; Peyrot, C.; Allais, F. *Green Chem.* **2020,** *22*, 2077–2085. doi:10.1039/D0GC00122H.

[12] Horbury, M.D.; Holt, E.L.; Mouterde, L.M.M.; Balaguer, P.; Cebrian, J.; Blasco, L.; Allais, F.; Stavros, V.G. *Nat. Commun.* **2019,** *10*, 1–8. doi:10.1038/s41467-019-12719-z.

[13] Dean, J.C.; Kusaka, R.; Walsh, P.S.; Allais, F.; Zwier, T.S. *J. Am. Chem. Soc.* **2014,** *136*, 14780–14795. doi:10.1021/ja5059026.

[14] Rioux, B.; Pinon, A.; Gamond, A.; Martin, F.; Laurent, A.; Champavier, Y.; Barette, C.; Liagre, B.; Fagnère, C.; Sol, V.; Pouget, C. *Eur. J. Med. Chem.* **2021,** *222*, 113586. doi:10.1016/j.ejmech.2021.113586.

[15] Rioux, B.; Pouget, C.; Fidanzi-Dugas, C.; Gamond, A.; Laurent, A.; Semaan, J.; Pinon, A.; Champavier, Y.; Leger, D.Y.; Liagre, B.; Duroux, J.-L.; Fagnere, C.; Sol, V. *Bioorg. Med. Chem. Lett.* **2017,** *27*, 4354–4357. doi:10.1016/j.bmcl.2017.08.024.

[16] Rioux, B.; Pouget, C.; Ndong-Ntoutoume, G.M.A.; Granet, R.; Gamond, A.; Laurent, A.; Pinon, A.; Champavier, Y.; Liagre, B.; Fagnere, C.; Sol, V. *Bioorg. Med. Chem. Lett.* **2019,** *29*, 1895–1898. doi:10.1016/j.bmcl.2019.05.056.

[17] Peyrot, C.; Mention, M.M.; Fournier, R.; Brunissen, F.; Couvreur, J.; Balaguer, P.; Allais, F. *Green Chem.* **2020,** *22*, 6510–6518. doi:10.1039/D0GC02763D.

[18] Ashraf, J.; Mughal, E.U.; Sadiq, A.; Bibi, M.; Naeem, N.; Ali, A.; Massadaq, A.; Fatima, N.; Javid, A.; Zafar, M.N.; Khan, B.A.; Nazar, M.F.; Mumtaz, A.; Tahir, M.N.; Mirzaei, M. *J. Biomol. Struct. Dyn.* **2020,** 1–16. doi:10.1080/07391102.2020.1805364.

[19] Balakrishna, M.; Kaki, S.S.; Karuna, M.S.L.; Sarada, S.; Kumar, C.G.; Prasad, R.B.N. *Food Chem.* **2017,** *221*, 664–672. doi:10.1016/j.foodchem.2016.11.121.

[20] Mouterde, L.M.M.; Allais, F. *Front. Chem.* **2018,** *6*, 426. doi:10.3389/fchem.2018.00426.

[21] Peyrot, C.; Peru, A.A.M.; Mouterde, L.M.M.; Allais, F. *ACS Sustainable Chem. Eng.* **2019,** *7*, 9422–9427. doi:10.1021/acssuschemeng.9b00624.

[22] Knoevenagel, E. *Ber. Dtsch. Chem. Ges.* **1894,** *27*, 2345–2346. doi:10.1002/cber.189402702229.

[23] Anastas, P.; Warner, J. *Green Chemistry: Theory and Practice*; Oxford Univ Press, 1998.

[24] Pollock, L.J.; Finkelman, I.; Arieff, A.J. *Arch. Intern. Med.* **1943,** *71*, 95–106. doi:10.1001/archinte.1943.00210010101008.

[25] Singh, P.; Kaur, M. *Chem. Commun.* **2011,** *47*, 9122–9124. doi:10.1039/C1CC12668G.

[26] Hedge, J.A.; Kruse, C.W.; Snyder, H.R. *J. Org Chem.* **1961,** *26*, 3166–3170. doi:10.1021/jo01067a032.

[27] Shi, D.; Wang, Y.; Lu, Z.; Dai, G. *Synth. Commun.* **2000,** *30*, 713–726. doi:10.1080/00397910008087374.

[28] Hu, X.; Ngwa, C.; Zheng, Q. *Curr. Org. Synth.* **2016,** *13*, 101–110. doi:10.2174/1570179412666150505185134.

[29] Forbes, D.C.; Law, A.M.; Morrison, D.W. *Tetrahedron Lett.* **2006,** *47*, 1699–1703. doi:10.1016/j.tetlet.2006.01.059.

[30] Hangarge, R.V.; Jarikote, D.V.; Shingare, M.S. *Green Chem.* **2002,** *4*, 266–268. doi:10.1039/b111634 g.

[31] Rajput, J.K.; Kaur, G. *Chin. J. Catal.* **2013,** *34*, 1697–1704. doi:10.1016/S1872-2067(12)60646-9.

[32] Isobe, K.; Hoshi, T.; Suzuki, T.; Hagiwara, H. *Mol. Diversity* **2005,** *9*, 317–320. doi:10.1007/s11030-005-8107-0.

[33] van Schijndel, J.; Canalle, L.A.; Molendijk, D.; Meuldijk, J. *Green Chemistry Letters and Reviews* **2017,** *10*, 404–411. doi:10.1080/17518253.2017.1391881.

[34] G. Thirupathi, M. Venkatanarayana, P. K. Dubey and Y. B. Kumari, *Org. Chem. Int.,* **2012,** 2012, 191584 doi:10.1155/2012/191584.

[35] Bukhari, S.N.A.; Jasamai, M.; Jantan, I.; Ahmad, W. *Mini-Rev. Org. Chem.* **2013,** *10*, 73–83. doi:10.2174/1570193X11310010006.

[36] Khan, M.U.; Aslam, M.; Shahzad, S.A.; Khan, Z.A.; Khan, N.A.; Ali, M.; Naz, S.; Rahman, J.; Farooq, U. *J. Mol. Struct.* **2021,** *1231*, 129959. doi:10.1016/j.molstruc.2021.129959.

[37] Lee, S.Y.; Slagle-Webb, B.; Sharma, A.K.; Connor, J.R. *Anticancer Res.* **2021,** *41*, 1171. doi:10.21873/anticanres.14874.

[38] Lu, W.; Xiong, H.; Chen, Y.; Wang, C.; Zhang, H.; Xu, P.; Han, J.; Xiao, S.; Ding, H.; Chen, Z.; Lu, T.; Wang, J.; Zhang, Y.; Yue, L.; Liu, Y.-C.; Zhang, C.; Yang, Y.; Jiang, H.; Chen, K.; Zhou, B.; Luo, C. *Bioorg. Med. Chem.* **2018,** *26*, 5397–5407. doi:10.1016/j.bmc.2018.07.048.

[39] Cagno, V.; Tintori, C.; Civra, A.; Cavalli, R.; Tiberi, M.; Botta, L.; Brai, A.; Poli, G.; Tapparel, C.; Lembo, D.; Botta, M. *PLOS ONE* **2018,** *13*, e0208333. doi:10.1371/journal.pone.0208333.

[40] Kadoma, Y.; Fujisawa, S. *Polymers. (Basel)* **2012,** *4*. doi:10.3390/polym4021025.

[41] Parameswaran, K.; Sivaguru, P.; Lalitha, A. *Bioorg. Med. Chem. Lett.* **2013,** *23*, 3873–3878. doi:10.1016/j.bmcl.2013.04.068.

[42] Raunio, H. *Front. Pharmacol.* **2011,** *2*. doi:10.3389/fphar.2011.00033.

[43] Myatt, G.J.; Ahlberg, E.; Akahori, Y.; Allen, D.; Amberg, A.; Anger, L.T.; Aptula, A.; Auerbach, S.; Beilke, L.; Bellion, P.; Benigni, R.; Bercu, J.; Booth, E.D.; Bower, D.; Brigo, A.; Burden, N.; Cammerer, Z.; Cronin, M.T.D.; Cross, K.P.; Custer, L.; Dettwiler, M.; Dobo, K.; Ford, K.A.; Fortin, M.C.;

Gad-McDonald, S.E.; Gellatly, N.; Gervais, V.; Glover, K.P.; Glowienke, S.; Van Gompel, J.; Gutsell, S.; Hardy, B.; Harvey, J.S.; Hillegass, J.; Honma, M.; Hsieh, J.-H.; Hsu, C.-W.; Hughes, K.; Johnson, C.; Jolly, R.; Jones, D.; Kemper, R.; Kenyon, M.O.; Kim, M.T.; Kruhlak, N.L.; Kulkarni, S.A.; Kümmerer, K.; Leavitt, P.; Majer, B.; Masten, S.; Miller, S.; Moser, J.; Mumtaz, M.; Muster, W.; Neilson, L.; Oprea, T.I.; Patlewicz, G.; Paulino, A.; Lo Piparo, E.; Powley, M.; Quigley, D.P.; Reddy, M.V.; Richarz, A.-N.; Ruiz, P.; Schilter, B.; Serafimova, R.; Simpson, W.; Stavitskaya, L.; Stidl, R.; Suarez-Rodriguez, D.; Szabo, D.T.; Teasdale, A.; Trejo-Martin, A.; Valentin, J.-P.; Vuorinen, A.; Wall, B.A.; Watts, P.; White, A.T.; Wichard, J.; Witt, K.L.; Woolley, A.; Woolley, D.; Zwickl, C.; Hasselgren, C. *Regul. Toxicol. Pharmacol.* **2018,** *96*, 1–17. doi:10.1016/j.yrtph.2018.04. 014.

[44] Mishra, K.; Ojha, H.; Chaudhury, N.K. *Food Chem.* **2012,** *130*, 1036–1043. doi:10.1016/j.foodchem.2011.07.127.

[45] Frenzel, F.; Buhrke, T.; Wenzel, I.; Andrack, J.; Hielscher, J.; Lampen, A. *Arch. Toxicol.* **2017,** *91*, 3157–3174. doi:10. 1007/s00204-016-1924-3.

[46] Glück, J.; Buhrke, T.; Frenzel, F.; Braeuning, A.; Lampen, A. *Food Chem. Toxicol.* **2018,** *116*, 298–306. doi:10.1016/j.fct. 2018.04.024.

[47] TEST, https://www.epa.gov/chemical-research/toxicity-estimation-software-tool-test (last accessed October 5, 2021).

[48] VEGA, https://www.vegahub.eu/portfolio-item/vega-qsar/ (last accessed October 5, 2021).

[49] LAZAR, https://lazar.in-silico.ch/predict (last accessed October 5, 2021).

[50] ISIDA/Predictor, http://infochim.u-strasbg.fr/cgi-bin/ predictor_reach.cgi (last accessed October 5, 2021).

[51] Llewellyn, B.A.; Davies, E.S.; Pfeiffer, C.R.; Cooper, M.; Lewis, W.; Champness, N.R. *Chem. Commun. (Cambridge, U. K.)* **2016,** *52*, 2099–2102. doi:10.1039/C5CC09962E.

[52] Kaupp, G.; Naimi-Jamal, M.R.; Schmeyers, J. *Tetrahedron* **2003,** *59*, 3753–3760. doi:10.1016/S0040-4020(03)00554-4.

[53] Hapiot, P.; Neudeck, A.; Pinson, J.; Fulcrand, H.; Neta, P.; Rolando, C. *J. Electroanal. Chem.* **1996,** *405*, 169–176. doi:10.1016/0022-0728(95)04412-4.

[54] Schallreuter, K.U.; Wood, J.M.; Farwell, D.W.; Moore, J.; Edwards, H.G.M. *J. Invest. Dermatol.* **1996,** *106*, 583–586. doi:10.1111/1523-1747.ep12344991.

[55] Ouchene, L.; Litvinov, I.V.; Netchiporouk, E. *J. Cutan. Med. Surg.* **2019,** *23*, 648–649. doi:10.1177/1203475419871592.

[56] Whysner, J.; Ross, P.M.; Williams, G.M. *Pharmacol. Ther.* **1996,** *71*, 153–191. doi:10.1016/0163-7258(96)00067-8.

[57] World Health Organization Model List of Essential Medicines, 21st List, 2019. Geneva: World Health Organization; 2019. Licence: CC BY-NC-SA 3.0 IGO https://apps.who.int/iris/handle/10665/325771 (last access: October 5, 2021).

[58] IARC, 2001, Volume 79, https://publications.iarc.fr/97 (last access: October 5, 2021).

[59] Elcombe, C.R.; Peffer, R.C.; Wolf, D.C.; Bailey, J.; Bars, R.; Bell, D.; Cattley, R.C.; Ferguson, S.S.; Geter, D.; Goetz, A.; Goodman, J.I.; Hester, S.; Jacobs, A.; Omiecinski, C.J.; Schoeny, R.; Xie, W.; Lake, B.G. *Crit. Rev. Toxicol.* **2014,** *44*, 64–82. doi:10.3109/10408444.2013.835786.

[60] Braeuning, A.; Gavrilov, A.; Geissler, M.; Wenz, C.; Colnot, S.; Templin, M.F.; Metzger, U.; Römer, M.; Zell, A.; Schwarz, M. *Arch. Toxicol.* **2016,** *90*, 1481–1494. doi:10. 1007/s00204-016-1667-1.

[61] Daré, R.G.; Oliveira, M.M.; Truiti, M.C.T.; Nakamura, C.V.; Ximenes, V.F.; Lautenschlager, S.O.S. *J. Photochem. Photobiol., B* **2020,** *203*, 111771. doi:10.1016/j. jphotobiol.2019.111771.

[62] Pillai, S.; Oresajo, C.; Hayward, J. *Int. J. Cosmet. Sci.* **2005,** *27*, 17–34. doi:10.1111/j.1467-2494.2004.00241.x.

[63] Rice-Evans, C.; Miller, N.J.; Paganga, G. *Free Radical Biol. Med.* **1996,** *20*, 933–956. doi:10.1016/0891-5849(95)02227-9.